Citation: BoneKEy Reports **5**, Article number: 837 (2016) | doi:10.1038/bonekey.2016.61

www.nature.com/bonekey

LABORATORY METHODS

Intramembranous bone regeneration and implant placement using mechanical femoral marrow ablation: rodent models

Meghan M Moran[1], Kotaro Sena[2], Margaret A McNulty[3], DR Sumner[1] and Amarjit S Virdi[1]

[1]Department of Anatomy and Cell Biology, Rush University Medical Center, Chicago, IL, USA. [2]Department of Periodontology, Kagoshima University, Kagoshima, Japan. [3]Department of Comparative Biomedical Sciences, Louisiana State University School of Veterinary Medicine, Baton Rouge, LA, USA.

In this paper, we provide a detailed protocol for a model of long bone mechanical marrow ablation in the rodent, including surgical procedure, anesthesia, and pre- and post-operative care. In addition, frequently used experimental end points are briefly discussed. This model was developed to study intramembranous bone regeneration following surgical disruption of the marrow contents of long bones. In this model, the timing of the appearance of bone formation and remodeling is well-characterized and therefore the model is well-suited to evaluate the *in vivo* effects of various agents which influence these processes. When biomaterials such as tissue engineering scaffolds or metal implants are placed in the medullary cavity after marrow ablation, end points relevant to tissue engineering and implant fixation can also be analyzed. By sharing a detailed protocol, we hope to improve inter-laboratory reproducibility.

BoneKEy Reports **5**, Article number: 837 (2016) | doi:10.1038/bonekey.2016.61

Introduction

There are several bone repair models currently in use, including fracture healing,[1,2] marrow ablation,[3–9] calvarial defect,[10,11] distraction osteogenesis,[8,12] segmental replacement[13] and spinal fusion.[14,15] Model choice depends upon the type of bone formation to be studied, as well as the importance of load-bearing, skeletal region and ability to translate to the clinic. The marrow ablation model is primarily used for two main purposes: (1) as a model for intramembranous bone regeneration[3,4,16,17] and (2) as a model to study implant fixation in orthopedics[9,18–21] and dentistry.[22,23] Therefore, the model is of interest to orthopedic and dental research, including biomaterial specialists, implant designers and molecular biologists as well as the field of regenerative medicine.

Bone regeneration occurs through either the endochondral or the intramembranous bone formation pathway. Endochondral bone forms from a cartilaginous precursor anlagen that is replaced by bone and is essential for most types of fracture repair.[24] Intramembranous bone is formed directly from mesenchymal cell condensations without any cartilage precursor. This latter pathway, although also present in fracture repair, is integral to bone defect repair, distraction osteogenesis and implant fixation.[9,25,26] Like nearly all wound repair responses, intramembranous bone formation following marrow ablation has inflammatory, repair and remodeling phases each of which are time-dependent, characterized histologically and genetically.[4] These phases for intramembranous bone formation are distinct from endochondral-based fracture repair. For instance, bone formation following marrow ablation, unlike endochondral-based fracture repair, does not include chondrocytes and lacks collagen type II mRNA expression.[27]

The marrow ablation model, used for nearly 70 years, was originally established in 1946 as an experimental model to study marrow regeneration in rabbits.[28] The first marrow ablation procedure used sterile mineral oil to flush out the marrow contents and a rigid metal probe to break-up the intramedullary bone. The debris was then flushed out with sterile saline through holes drilled in the diaphysis. Suva *et al.*[7] were the first to use a needle to manually disrupt or ablate the marrow contents during marrow ablation surgery.[7] Later the use of a needle was continued, but the use of a dental brush was added to further remove marrow contents, combined with flushing with sterile saline.[29] Our lab first used the Suva *et al.*[7] method of marrow ablation[7] to study gene expression during intramembranous

Correspondence: Dr AS Virdi, Department of Anatomy and Cell Biology, Rush University Medical Center, Chicago, IL 60612, USA.
E-mail: amarjit_virdi@rush.edu

Received 10 March 2016; accepted 19 July 2016; published online 7 September 2016

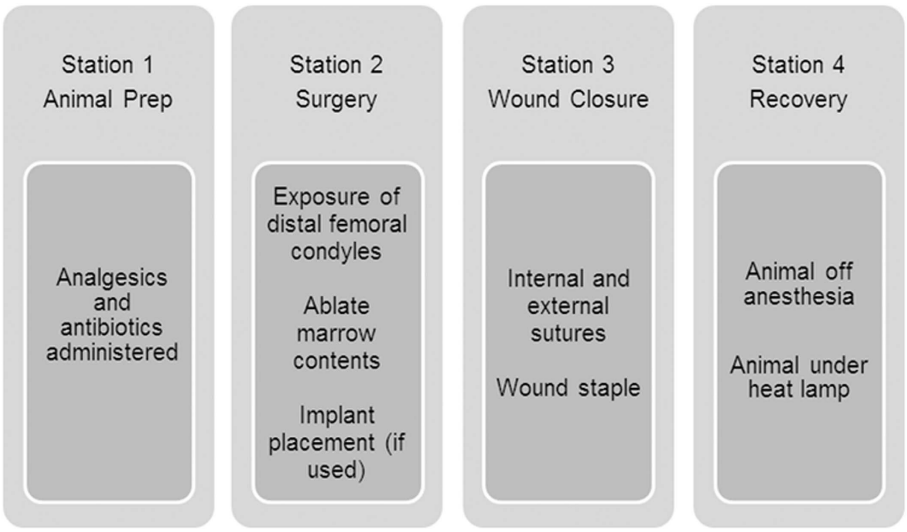

Figure 1 Workflow schematic for rodent marrow ablation surgery. The four stations and associated tasks for marrow ablation surgery are outlined here.

bone regeneration,[5] and incorporated surgical aspects as used by Bab[6] in both a gene-expression study[4] and a drug treatment study.[3] Our lab and several others have used the marrow ablation model with the addition of an implant to study implant fixation.[4,9,18,30,31]

In addition to providing a specific platform to study post-injury intramembranous bone formation, the mechanical marrow ablation model is a technique that is applicable to clinical medicine. It mimics the surgical process of intramedullary ablation required prior to implant placement during joint replacement surgery in humans. The prevalence of total knee arthroplasty and total hip arthroplasty increased by 6% from 2009–2010.[32] Perhaps, more importantly, the number of people requiring joint replacement is expected to increase by over 100% in the next 15 years and those people needing revision surgery will double by 2026.[33] There is a great need for dental implants as well with about 450 000 osseointegrated dental implants being placed each year.[34] With increased medical need for joint replacement and dental implants, a robust, reproducible pre-clinical model can contribute to testing new therapies and better the understanding of implant healing and physiology. Thus, there is a clear need for standardization of research tools such as the mechanical marrow ablation model.

The mechanical marrow ablation model is an animal model used to study post-injury intramembranous bone repair, biomaterial compatibility and implant fixation. In this paper, we provide a detailed protocol for marrow ablation in mice and marrow ablation with implant placement in rats. Our discussion describes several methods to evaluate the post-ablation bone regeneration and bone-implant contact including micro-computed tomography (μCT), mechanical pull-out testing, histology, dynamic histomorphometry, gene expression and biomarkers. Any of these study end points can be used in this model and may be translatable to clinical measures.

Materials and Methods

Using the team-based approach described here, the femoral marrow ablation surgery takes ~1 h for 8 mice (each mouse is anesthetized for about 7 min) and marrow ablation with implant placement in rats takes ~1 h for 6 rats (each rat is anesthetized for about 10 min). The length of time is important to track to ensure animals are not under anesthesia for too long.

Pre-operative preparation for marrow ablation

Team composition. For optimal surgery outcomes, a six-person surgery team is organized with four work stations (**Figure 1**). In station 1, the technician anesthetizes, prepares the animal for surgery and administers analgesic, antibiotics and fluids prior to surgery; this way the drugs are in the animal's system prior to the start of surgery. In station 2, the surgeon and surgical assistant complete the ablation surgery and, when used, implant or biomaterial placement. In station 3, the wound is sutured by the closer and the closer assistant. The animal is then moved to station 4 for recovery under a heat lamp. Procedures at stations 2 and 3 occur under sterile conditions. A non-sterile assistant is helpful to move animals between stations and to ensure that an anesthetic plane is maintained during surgery.

Preparation. The animals are ordered at least 3 weeks prior to surgery to allow for quarantine which varies per institution and, if necessary, aging. We use this technique on multiple inbred and outbred mouse strains (Jackson Laboratories, Bar Harbor, ME, USA: FVB/NJ, C3H/HeJ, C57Bl/6 J, BALB/cJ and Charles River, Kingston, NY, USA: Swiss Webster) and skeletally mature, 400 g rats (Envigo Medical Laboratory, Madison, WI, USA and Charles River: Sprague–Dawley).

Prior to surgery, surgical supplies are sterilized (see the 'Materials and methods' section). All surgical tools, emesis basins, gauze and drapes are placed on stainless steel trays (organized per surgical station) and wrapped in separate drapes. These packages are secured with autoclave tape and autoclaved on the dry cycle, lasting about 1 h. In total, supplies tend to be autoclaved in 2–3 wrapped packages. Animals are weighed to establish baseline, pre-surgery weights. Pre-surgery weights are used to calculate per animal dosages of any drugs administered as part of the experimental design. For mice and rats buprenorphine (0.05 mg kg^{-1}) can be used

for analgesia and gentamicin (5 mg kg^{-1}) for antibiotic; other drugs can be substituted depending on DEA licensing and IACUC protocol per institution.

Materials
- Sterile tools
- Iris scissors
- Dumont forceps
- Straight-tip forceps
- Needle holders
- Scalpel handles
- Wound closure stapler and staples
- Emesis basins
- 2 × 2 in gauze
- Surgical drape
- Sterile saline
- 70% EtOH
- Betadine
- Isoflurane liquid inhalation
- Isoflurane vaporizer and filter
- Rodent induction chamber
- Buprenorphine
- Gentamicin
- 10% neutral buffered formalin
- Scalpel blades
- 5-0 MONOCRYL Suture
- 3 cc insulin syringes with 29 g needle
- Heat lamp
- Small animal scale
- Ear tag applicator and ear tags
- Electric razor
- Heat pad for surgery table
- Petroleum eye ointment
- Bevel edge needle 23 g
- Bevel edge needle 25 g
- Bevel edge needle 30 g
- 1 ml syringe
- Bone wax

For rat marrow ablation and implant placement
- Dremel drill (battery powered)
- Drill bits
- 10 ml syringes with 25 g needles for flushing
- 15 mm long × 1.5 mm diameter titanium rods
- 4 × 4 in gauze

Procedure for mechanical marrow ablation in mouse

Marrow ablation surgery takes about 8 min per animal. At the first station, the animal is anesthetized; isoflurane gas or ketamine are two options for anesthesia.[35] Test for the withdrawal reflex by pinching the paw of the animal; if there is not a reflexive flexion of the limb, the animal is non-responsive to noxious stimuli and is deeply sedated. Once the animal is safely sedated, the operable leg is prepared for surgery. The operable leg is shaved and then scrubbed with Betadine and 70% ethanol to sterilize the operable region, as reported previously.[4,9]

The animal is moved to the second station on the surgery table and placed on a heating pad to avoid an anesthesia induced drop in body temperature. Careful attention to maintenance of sedation is achieved by periodically repeating the paw pinch test. The animal is draped for surgery. Using aseptic technique, surgery begins with a small longitudinal skin incision along the medial knee joint, ~1 cm long, which exposes the 1.5 mm long white patellar tendon running longitudinally superficial to the knee joint (**Figure 2a**). A second incision is made deep to the first at the medial border of the patellar tendon. The surgery assistant carefully moves the patellar tendon laterally using Dumont forceps. Note, straighten the knee while moving the tendon laterally to lessen the risk of tearing the tendon from its muscular attachments. The glossy, cartilage-covered distal femoral condyles are now exposed (**Figure 2b**). Using a 25 g bevel edge needle or a similar sized drill bit, the surgeon gains access to the medullary canal by repeatedly twisting the needle/bit clockwise and counter-clockwise in the femoral intercondylar fossa (**Figure 2c**).

To ream the intramedullary contents, a 23 g bevel edge needle or a similar sized drill bit, is placed in the newly formed ablation site. The needle/bit is pistoned in and out of the intramedullary canal and turned clockwise and counter-clockwise. During reaming, the surgeon may feel a 'crunchy' texture as the trabecular bone is broken up. The lesser trochanter is the proximal limit to reaming; progressing proximal to the lesser trochanter risks breaking through the proximal end of the femur. Once the intramedullary contents are sufficiently disrupted the needle/drill bit glides easily in and out of the medullary canal. The ablation site is then flushed with 0.6 ml of warmed sterile saline. The dislodged intramedullary contents are visible flowing out of the ablation site as bright red debris. Flushing is an optional step in the ablation process depending on the desired end points of the experiment.[9] After flushing, the access site can be filled with sterile bone wax closing off the intramedullary canal from the joint space (**Figure 2d**). Only a small amount of wax is needed to seal the hole and ebb bleeding. To set the wax in place, use the flat side of the scalpel blade or the back end of the scalpel handle to flatten the wax into place. Finally, wipe the distal femur with a piece of sterile gauze to remove any bone wax fragments.

After marrow ablation, the animal is moved to the third station for wound closure. Sutures are placed internally to reposition the patellar tendon and externally to close the skin. A wound staple is placed over the external sutures to protect them from being chewed or scratched out (**Figure 2e**). Care must be taken to avoid clamping the medial saphenous vein within the wound clip, which will result in extensive swelling of the distal limb.

After the wound is closed, the non-sterile assistant moves the animal to the fourth station for recovery. The animal is placed under a heat lamp and recovers from anesthesia. Note, all cage mates should be kept together as to not stress the animals unnecessarily.

Post-operative management and analgesia for mice

On post-operative day 1, antibiotic and analgesic injections are administered subcutaneously to each animal. The same doses are administered as on surgery day. The surgical wounds are checked for any disruption and, if need be, wounds are re-sutured or wound clips are replaced.

On post-operative day 2, antibiotics are administered subcutaneously to each animal, and if necessary adequate analgesics are administered. Analgesic administration is based on the presence of pain behaviors such as hypo-locomotion, paw lifting, guarding of operated limb and lack of grooming.[36] Our experience is that these behaviors are rare by post-operative day 2.

Pre-operative preparation for marrow ablation and implant placement in the rat

The same pre-operative procedures are followed for rats as for mice. In short, a six-person surgery team is organized. Animals

are ordered with enough time to account for quarantine and potential aging. Surgical tools are prepared, pre-operative animal weights are recorded and drug dosages are calculated and drawn up into syringes. Note, Larger, 4×4 in, gauze is best to use in rat surgery instead of the 2×2 in gauze used for mice.

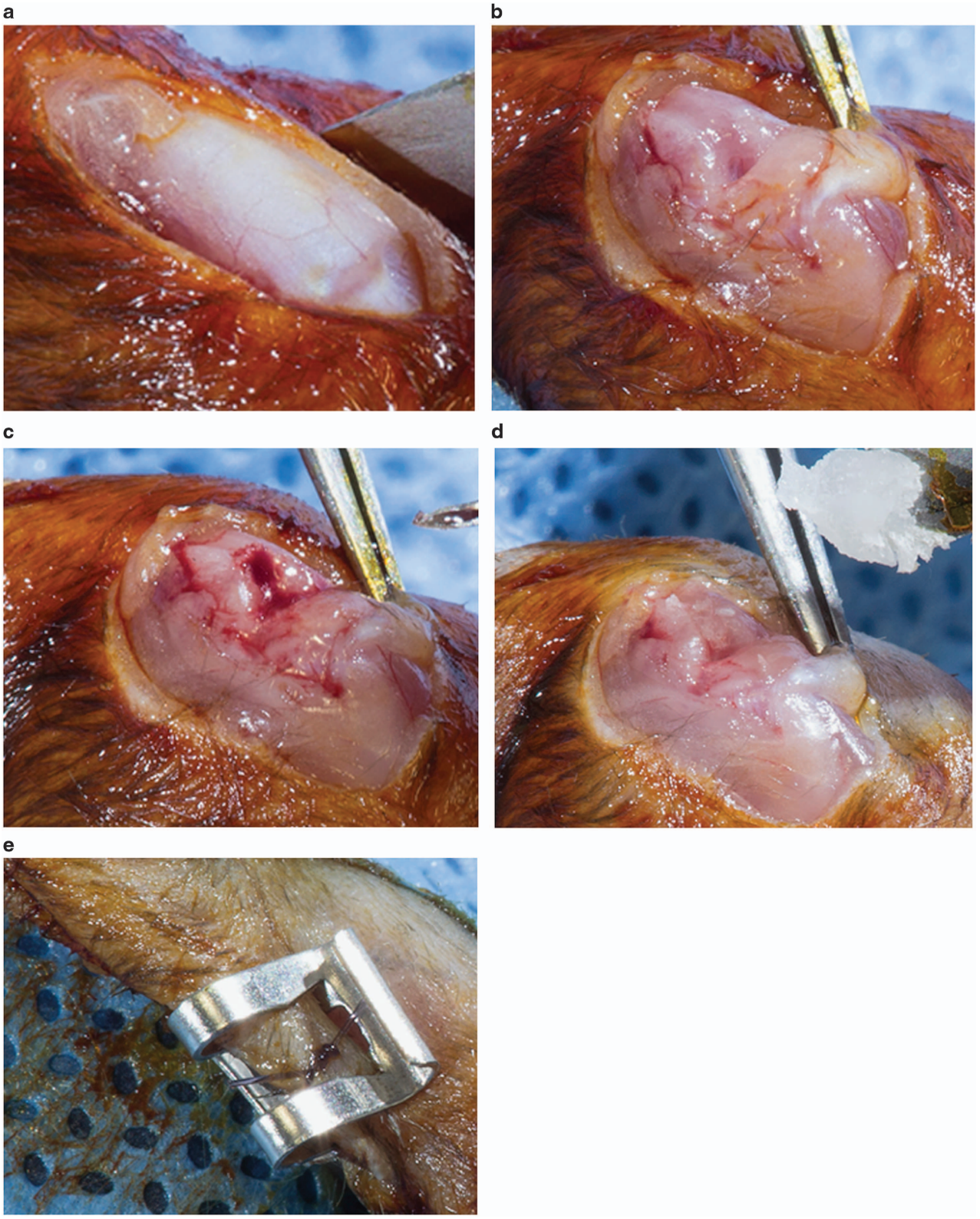

Figure 2 Mouse marrow ablation surgery. (**a**) skin incision, (**b**) exposure of distal femoral condyles, (**c**) mechanical marrow ablation complete, (**d**) ablation site sealed with bone wax and (**e**) final closure with staple.

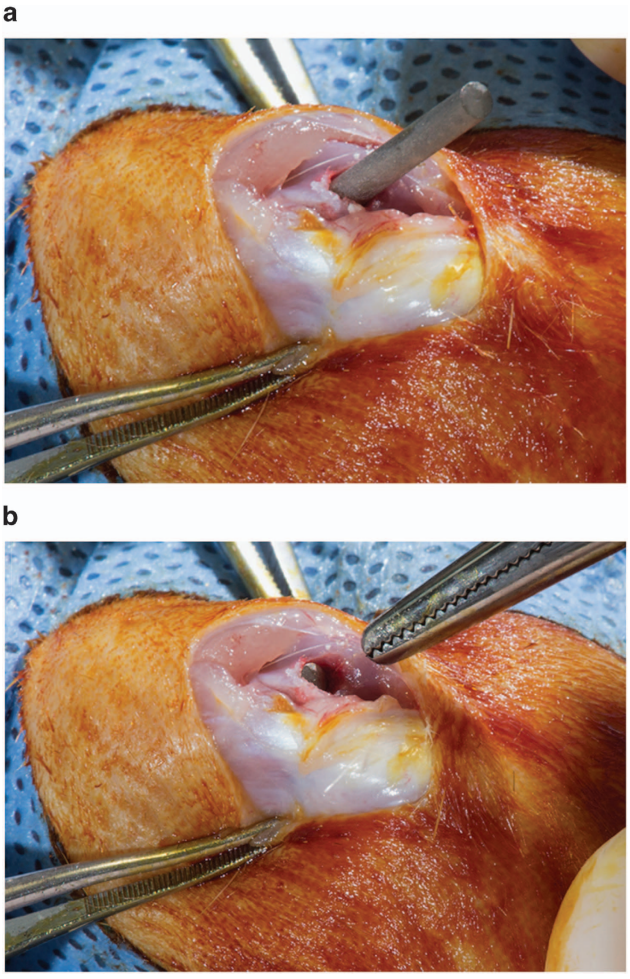

Figure 3 Rat implant placement. (**a**) implant placement in ablation site at distal femur and (**b**) implant sunk deep to articular surface.

Procedure for mechanical marrow ablation and implant placement in rats

Marrow ablation surgery and implant placement takes about 10 min per rat. Rats are anesthetized using an intra-abdominal injection of ketamine (100 mg kg^{-1}) and xylazine (5 mg kg^{-1}). This anesthesia is administered 10 min prior to the start of surgery. Once injected with anesthesia, the rats are prepared for surgery the same way as the mice.

The same mechanical marrow ablation steps (**Figure 2**) are completed in the rat with one difference. A battery-operated Dremel tool is used to gain access to the medullary canal through the intercondylar fossa. The subchondral bone in rats is hard and the extra force of a drill is needed to penetrate it. The intramedullary canal is reamed by hand using a drill bit with a handle. The exact size of the drill bits depends upon the study. In our lab, we often place a 1.5 mm diameter implant into the reamed cavity and, typically use a 1.6 mm drill bit to break through the subchondral bone and a 1.5 mm drill bit for reaming.

Once the intramedullary canal is reamed, there are different scenarios available depending on end points of the experiment. The first is the same as described above in the mouse model, where the marrow space is flushed and the access site is capped with bone wax.[4] A second scenario involves implant placement whereby the marrow space can be flushed and an implant is hand fit into the canal until it is just deep to the joint surface (**Figure 3**). Depending upon the study, the opening with implant present can be filled with bone wax.[19] A third scenario uses a larger hand drill with a 2.0 mm drill bit to widen the distal 5 mm of the ablation site, followed by implant placement.[20] This widened portion of the canal and the lack of bone wax allow for exposure of the ablation site to the joint space and is used in a model where particles are introduced into the joint space to mimic particle-induced peri-implant osteolysis.[20] Suturing and surgical staple placement are completed in the same manner as in the mouse surgery.

Post-operative management and analgesia for rats

Post-operative care is the same for rats as previously discussed in mice.

Reproducibility of surgery outcomes

We have employed this model in a number of studies.[4,17,20,21,37,38] To assess the reproducibility of the model, we re-analyzed outcome data from the mouse marrow ablation model and the rat implant fixation model in which the animal strain, age, sex and experimental end points were comparable. Both mouse studies included females from FVB/NJ and BALB/cJ strains of the same age (10–11 weeks) with the same end point (bone volume/tissue volume, BV/TV) at 7 days post-marrow ablation. For study 1,[17] the within-study coefficient of variation (s.d./mean $\times$ 100%) was 40% for FVB/NJ and 60% for BALB/c. For study 2 (unpublished) the coefficient of variation was 60% for FVB/NJ and 63% for BALB/c. Mean values for BV/TV between study 1 and study 2 were not different for either FVB/NJ ($P = 0.977$) or BALB/cJ ($P = 0.386$, Student's t-test). Levene's test for equality of variances showed no significant difference for BV/TV between the two studies (FVB/N, P-value $= 0.437$ and BALB/c, P-value $= 0.311$).

Similarly, we compared comparable groups from two studies using the rat implant model,[20,21] in which 6-month old male Sprague–Dawley rats had implants in place for 12 weeks. In this case, we examined the mechanical strength of implant fixation within the host bone. The within-study coefficient of variation for implant fixation was 29% for control samples and 30% for animals treated with polyethylene particles in the first study[20] and 34% for control and 51% for particle-treated animals in the second study.[21] The mean strength of implant fixation did not vary for the control groups (P-value $= 0.065$) or particle-treated groups (P-value $= 0.283$) between the two studies. Levene's test for equality of variances also showed no significant difference in fixation strength between study 1 and study 2 (control groups, P-value $= 0.970$ and polyethylene treated groups, P-value $= 0.557$). Together, these analyses indicate that the marrow ablation model is a reproducible surgical model for studying bone regeneration and implant fixation.

Discussion

The outcomes of the mechanical marrow ablation model are reproducible and applicable to the study of intramembranous bone regeneration[3,4,16] and bone-implant fixation in orthopedic[9,18,19] and dental[22,23] applications. As a technique with a bone regeneration end point (**Figure 4**), the marrow ablation model induces trabecular bone formation within the

intramedullary canal in regions that, under normal conditions, lack trabecular bone. The regenerated bone induced by this model is specifically intramembranous bone,[6,39] as opposed to fracture models where the endochondral bone formation pathway is induced.[40] The marrow ablation model mimics the process of intramedullary reaming for implant placement during joint replacement surgery in humans.

The histological sequence of bone regeneration events from intact (no surgery) through 56 days post-surgery was previously published.[4] We showed that operated limbs exhibit bone formation within the ablated region as early as day 5 in the rat marrow ablation model and day 7 in the mouse marrow ablation model.[4,17] The newly formed intramedullary bone is resorbed and replaced by lamellar bone (that is, remodeled) beginning around day 10 post-ablation. Typically, the intramedullary contents return to baseline with few remaining trabeculae, if an implant has not been placed, between 28 and 56 days post-ablation.[4] The timing of these histological bone regeneration events is probably condensed in the rodent model compared to patients receiving joint replacements.[4,41–43] The model has proven useful in understanding principles relevant to bone regeneration,[4,17] bone-implant contact[9,18,19] and implant fixation.[30] and bone ingrowth.[44]

In vivo models are advantageous because of inherent limitation of *in vitro* studies. Several translational end points that are relevant to tissue engineering and implant fixation can be analyzed after mechanical marrow ablation, including behavioral testing, imaging by μCT, mechanical pull-out testing, histology, dynamic histomorphometry, gene expression and biomarkers.

Behavioral testing

Behavioral testing is important to evaluate the animal for pain or discomfort after the surgical procedure. We assayed ambulation and rearing with a photobeam activity system. This system consists of two sets of photobeams, one to measure ambulation and another to measure rearing.[45] Together these measurements calculate the animal's movements within its environment and are used as a functional test to compare treatments.

Micro-computed tomography

μCT is a non-invasive technique that yields a high-resolution three-dimensional image, in this case, of the post-operative regenerated intramedullary trabecular bone (**Figure 4**) or peri-implant bone within a designated region of interest. Cortical bone geometry can be assessed using μCT as well. Specimens are fixed in either 10% neutral buffered formalin, 70% ethanol, RNAlater or frozen at $-20\,^{\circ}C$ in saline soaked gauze. Detailed guidelines for scanning rodent bones and the definitions of μCT variables are established and should be followed.[46]

Mechanical pull-out testing

Mechanical pull-out testing determines the strength of fixation of the implant within the host skeleton. Specimens used for mechanical testing are wrapped in saline soaked gauze and frozen at $-20\,^{\circ}C$ so that testing of multiple specimens can be organized, although fresh specimens can be tested. End points for mechanical pull-out testing are implant fixation strength and may also include measures of stiffness and energy.[47]

Histology and dynamic histomorphometry

Histology shows the morphology of the tissue, including cell types present.[4] Most commonly, specimens are fixed in 10%

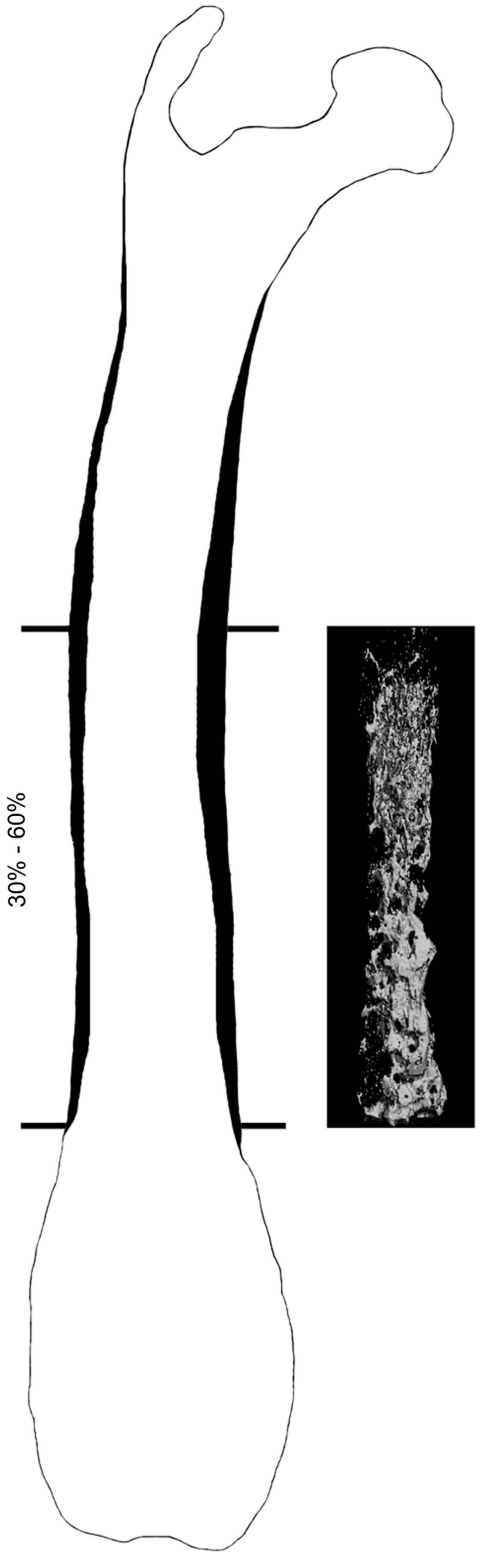

Figure 4 Region of interest, 30–60% of total femoral length. Three-dimensional rendering of post-ablation regenerated trabecular bone in a region that is normally devoid of bone.

neutral buffered formalin and prepared for decalcified or undecalcified histology as well as other techniques such as immunohistochemistry[48] for protein expression patterns or *in situ* hybridization for gene-expression patterns. If animals were administered flurochrome labels, dynamic histomorphometry may also be an end point to measure bone remodeling.[49,50]

Gene expression

Gene-expression profiling assesses the relative activity of genes within the tissue being studied and can give insights into molecular mechanisms.[4,51] Tissues should be harvested and immediately placed in RNAlater or an equivalent reagent to optimally preserve the RNA. Tissue is left in RNAlater at room temperature for 24 h and then frozen at $-20\,^{\circ}C$ to undergo RNA isolation and for microarray or next-generation sequencing.

Biomarkers

Biomarkers are measurable indicators of a process, for example bone formation or bone resorption that can be tested for in blood or other body fluids. Post-ablated, regenerated medullary contents or peri-implant tissue are two additional tissues that can be used to test for biomarker concentrations. If blood is used, it is typically collected *in vivo* via the tail vein or while killing via a cardiac puncture. Blood is then centrifuged to separate the serum from blood solids and serum samples are stored at $-20\,^{\circ}C$ until analyzed.[38]

Conclusion

This protocol provides a detailed description of the mechanical marrow ablation model as used in rodents for various applications. The mechanical marrow ablation technique provides a reproducible platform specific to studying intramembranous bone regeneration, post-injury bone healing, implant fixation or biomaterial performance. Publishing detailed protocols for techniques like this provides uniformity and helps ensure repeatability in method across laboratories. This will ultimately establish a standard which provides value in evaluating results across studies.

Conflict of Interest

The authors declare no conflict of interest.

Acknowledgements

Work described here was supported by the National Institute of Arthritis and Musculoskeletal and Skin Diseases of the National Institutes of Health under Award Numbers R21AR054171, T32AR052272, R21AR065604, R01AR066562 (the content is solely the responsibility of the authors and does not necessarily represent the official views of the National Institutes of Health), the Musculoskeletal Transplant Foundation and industry. The use of the Rush MicroCT/Histology Core Lab is recognized. Many trainees and colleagues contributed to these studies, including Aladino De Ranieri, MD, PhD who was instrumental in the early phases.

References

1. Manigrasso MB, O'Connor JP. Comparison of fracture healing among different inbred mouse strains. *Calcif Tissue Int* 2008; **82**: 465–474.
2. Gerstenfeld LC, Cullinane DM, Barnes GL, Graves DT, Einhorn TA. Fracture healing as a post-natal developmental process: molecular, spatial, and temporal aspects of its regulation. *J Cell Biochem* 2003; **88**: 873–884.
3. McNulty MA, Virdi AS, Christopherson KW, Sena K, Frank RR, Sumner DR. Adult stem cell mobilization to enhance intramembranous bone regeneration: a pilot study. *Clin Orthop Relat Res* 2012; **470**: 2503–2512.
4. Wise JK, Sena K, Vranizan K, Pollock JF, Healy KE, Hughes WF *et al.* Temporal gene expression profiling during rat femoral marrow ablation-induced intramembranous bone regeneration. *PLoS ONE* 2010; **5**: e12987.
5. Kuroda S, Virdi AS, Dai Y, Shott S, Sumner DR. Patterns and localization of gene expression during intramembranous bone regeneration in the rat femoral marrow ablation model. *Calcif Tissue Int* 2005; **77**: 212–225.
6. Bab IA. Postablation bone marrow regeneration: an *in vivo* model to study differential regulation of bone formation and resorption. *Bone* 1995; **17**: 437S–441S.
7. Suva LJ, Seedor JG, Endo N, Quartuccio HA, Thompson DD, Bab I *et al.* Pattern of gene expression following rat tibial marrow ablation. *J Bone Miner Res* 1993; **8**: 379–388.
8. Lybrand K, Bragdon B, Gerstenfeld L. Mouse models of bone healing: fracture, marrow ablation, and distraction osteogenesis. *Curr Protoc Mouse Biol* 2015; **5**: 35–49.
9. De Ranieri A, Virdi AS, Kuroda S, Healy KE, Hallab NJ, Sumner DR. Saline irrigation does not affect bone formation or fixation strength of hydroxyapatite/tricalcium phosphate-coated implants in a rat model. *J Biomed Mater Res B Appl Biomater* 2005; **74**: 712–717.
10. Cooper GM, Mooney MP, Gosain AK, Campbell PG, Losee JE, Huard J. Testing the critical size in calvarial bone defects: revisiting the concept of a critical-size defect. *Plast Reconstr Surg* 2010; **125**: 1685–1692.
11. Lee JH, Kim CS, Choi KH, Jung UW, Yun JH, Choi SH *et al.* The induction of bone formation in rat calvarial defects and subcutaneous tissues by recombinant human BMP-2, produced in Escherichia coli. *Biomaterials* 2010; **31**: 3512–3519.
12. Yu YY, Bahney C, Hu D, Marcucio RS, Miclau T III. Creating rigidly stabilized fractures for assessing intramembranous ossification, distraction osteogenesis, or healing of critical sized defects. *JVisExp* 2012; **11**: pii 3552.
13. Kumar S, Ponnazhagan S. Mobilization of bone marrow mesenchymal stem cells in vivo augments bone healing in a mouse model of segmental bone defect. *Bone* 2012; **50**: 1012–1018.
14. Boden SD, Schimandle JH. Biologic enhancement of spinal fusion. *Spine* 1995; **20**: 113S–123S.
15. Boden SD, Sumner DR. Biologic factors affecting spinal fusion and bone regeneration. *Spine* 1995; **20**: 102S–112S.
16. Gerstenfeld LC, Cho TJ, Kon T, Aizawa T, Tsay A, Fitch J *et al.* Impaired fracture healing in the absence of TNF-alpha signaling: the role of TNF-alpha in endochondral cartilage resorption. *J Bone Miner Res* 2003; **18**: 1584–1592.
17. Moran MM, Virdi AS, Sena K, Mazzone SR, McNulty MA, Sumner DR. Intramembranous bone regeneration differs among common inbred mouse strains following marrow ablation. *J Orthop Res* 2015; **33**: 1374–1381.
18. Kuroda S, Virdi AS, Li P, Healy KE, Sumner DR. A low temperature biomimetic calcium phosphate surface enhances early implant fixation in a rat model. *J Biomed Mater Res* 2004; **70A**: 66–73.
19. Virdi AS, Irish J, Sena K, Liu M, Ke HZ, McNulty MA *et al.* Sclerostin antibody treatment improves implant fixation in a model of severe osteoporosis. *J Bone Joint Surg* 2015; **97**: 133–140.
20. Liu S, Virdi AS, Sena K, Hughes WF, Sumner DR. Bone turnover markers correlate with implant fixation in a rat model using LPS doped particles to induce implant loosening. *J Biomed Mater Res A* 2012; **100A**: 918–928.
21. Liu S, Virdi AS, Sena K, Sumner DR. Sclerostin antibody prevents particle-induced implant loosening by stimulating bone formation and inhibiting bone resorption in a rat model. *Arthritis Rheum* 2012; **64**: 4012–4020.
22. Shibata Y, Tanimoto Y. A review of improved fixation methods for dental implants. Part I: Surface optimization for rapid osseointegration. *J Prosthodont Res* 2015; **59**: 20–33.
23. Yazicioglu D, Bayram B, Oguz Y, Cinar D, Uckan S. Stress Distribution on short implants at maxillary posterior alveolar bone model with different bone-to-implant contact ratio: finite element analysis. *J Oral Implantol* 2015; **42**: 26–33.
24. Mackie EJ, Ahmed YA, Tatarczuch L, Chen KS, Mirams M. Endochondral ossification: how cartilage is converted into bone in the developing skeleton. *Int J Biochem Cell Biol* 2008; **40**: 46–62.
25. Forriol F, Denaro L, Longo UG, Taira H, Maffulli N, Denaro V. Bone lengthening osteogenesis, a combination of intramembranous and endochondral ossification: an experimental study in sheep. *Strategies Trauma Limb Reconstr* 2010; **5**: 71–78.
26. Grimes R, Jepsen KJ, Fitch JL, Einhorn TA, Gerstenfeld LC. The transcriptome of fracture healing defines mechanisms of coordination of skeletal and vascular development during endochondral bone formation. *J Bone Miner Res* 2011; **26**: 2597–2609.
27. Liang CT, Barnes J, Seedor JG, Quartuccio HA, Bolander M, Jeffrey JJ *et al.* Impaired bone activity in aged rats: alterations at the cellular and molecular levels. *Bone* 1992; **13**: 435–441.
28. Steinberg B, Martin RA. Removal of bone marrow in living animals. *Proc Soc Exp Biol Med* 1946; **61**: 428.

29. Shimizu T, Mehdi R, Yoshimura Y, Yoshikawa H, Nomura S, Miyazono K *et al.* Sequential expression of bone morphogenetic protein, tumor necrosis factor, and their receptors in bone-forming reaction after mouse femoral marrow ablation. *Bone* 1998; **23**: 127–133.
30. Hara T, Hayashi K, Nakashima Y, Kanemaru T, Iwamoto Y. The effect of hydroxyapatite coating on the bonding of bone to titanium implants in the femora of ovariectomised rats. *J Bone Joint Surg* 1999; **81-B**: 705–709.
31. Sena K, Sumner DR, Virdi AS. Effect of recombinant human transforming growth factor-beta2 dose on bone formation in rat femur titanium implant model. *J Biomed Mater Res A* 2010; **92**: 1210–1217.
32. Kurtz SM, Ong KL, Lau E, Bozic KJ. Impact of the economic downturn on total joint replacement demand in the United States: updated projections to 2021. *J Bone Joint Surg* 2014; **96**: 624–630.
33. Kurtz S, Ong K, Lau E, Mowat F, Halpern M. Projections of primary and revision hip and knee arthroplasty in the United States from 2005 to 2030. *J Bone Joint Surg* 2007; **89**: 780–785.
34. Gaviria L, Salcido JP, Guda T, Ong JL. Current trends in dental implants. *J Korean Assoc Oral Maxillofac Surg* 2014; **40**: 50–60.
35. Flecknell PA. Anesthesia and perioperative care. *Methods Enzymol* 1993; **225**: 16–33.
36. Mogil JS, Crager SE. What should we be measuring in behavioral studies of chronic pain in animals? *Pain* 2004; **112**: 12–15.
37. Irish J, Virdi AS, Sena K, Liu M, Ke HZ, Sumner DR. Sclerostin antibody enhances bone-implant contact by increasing bone formation and inhibiting bone resorption. *Transactions of the Orthopaedic Research Society* 2012; **37**: 1499.
38. Ross RD, Virdi AS, Liu S, Sena K, Sumner DR. Particle-induced osteolysis is not accompanied by systemic remodeling but is reflected by systemic bone biomarkers. *J Orthop Res* 2014; **32**: 967–973.
39. Barber TA, Gamble LJ, Castner DG, Healy KE. *In vitro* characterization of peptide-modified p(AAm-co-EG/AAc) IPN-coated titanium implants. *J Orthop Res* 2006; **24**: 1366–1376.
40. Einhorn TA. The cell and molecular biology of fracture healing. *Clin Orthop Relat Res* 1998; **355S**: S7–S21.
41. Patt HM, Maloney MA. Bone marrow regeneration after local injury: a review. *Exp Hematol* 1975; **3**: 135–148.
42. Urban RM, Jacobs JJ, Sumner DR, Peters CL, Voss FR, Galante JO. The bone-implant interface of femoral stems with non-circumferential porous coating: a study of specimens retrieved at autopsy. *J Bone Joint Surg* 1996; **78-A**: 1068–1081.
43. Sumner DR, Jasty M, Jacobs JJ, Urban RM, Bragdon CR, Harris WH *et al.* Histology of porous-coated acetabular components: 25 cementless cups retrieved after arthroplasty. *Acta Orthop Scand* 1993; **64**: 619–626.
44. Barber TA, Ho J, De Ranieri A, Virdi AS, Sumner DR, Healy KE. Peri-implant bone formation and implant integration strength of peptide-modified p(AAm- co -EG/AAc) IPN coated titanium implants. *J Biomed Mater Res* 2007; **80A**: 306–320.
45. Piel MJ, Kroin JS, van Wijnen AJ, Kc R, Im HJ. Pain assessment in animal models of osteoarthritis. *Gene* 2014; **537**: 184–188.
46. Bouxsein ML, Boyd SK, Christiansen BA, Guldberg RE, Jepsen KJ, Muller R. Guidelines for assessment of bone microstructure in rodents using micro-computed tomography. *J Bone Miner Res* 2010; **25**: 1468–1486.
47. Turner CH, Burr DB. Basic biomechanical measurements of bone: a tutorial. *Bone* 1993; **14**: 595–608.
48. Pereira RC, Valta H, Tumber N, Salusky IB, Jalanko H, Makitie O *et al.* Altered osteocyte-specific protein expression in bone after childhood solid organ transplantation. *PLoS ONE* 2015; **10**: e0138156.
49. Wronski TJ, Ratkus AM, Thomsen JS, Vulcan Q, Mosekilde L. Sequential treatment with basic fibroblast growth factor and parathyroid hormone restores lost cancellous bone mass and strength in the proximal tibia of aged ovariectomized rats. *J Bone Miner Res* 2001; **16**: 1399–1407.
50. Erben RG, Glosmann M. Histomorphometry in rodents. *Methods Mol Biol* 2012; **816**: 279–303.
51. Elangovan S, D'Mello SR, Hong L, Ross RD, Allamargot C, Dawson DV *et al.* The enhancement of bone regeneration by gene activated matrix encoding for platelet derived growth factor. *Biomaterials* 2014; **35**: 737–747.